THE UNIVERSITY OF

WARWICK

warwickpublicationswrap

highlight your research

http://wrap.warwick.ac.uk

ARTICLE TYPE

Dissociation and Hierarchical Assembly of Chiral Esters on Metallic Surfaces

## Ben Moreton,[a] Zhijia Fang,[a] Martin Wills[a] and Giovanni Costantini*[a]

The interaction of a *de novo* synthesised ester with single crystal metal surfaces has been investigated as a model system for the heterogeneous hydrogenolysis of esters. Scanning tunnelling microscopy measurements show a dissociative adsorption at room temperature on Cu(110) but no significant reaction on Au(111). The dissociative pathway has been identified by comparing with possible fragment species, demonstrating that the ester cleavage occurs along the RCH(CH$_3$)-OC(O)R bond.

Scanning tunnelling microscopy (STM) has developed into a useful tool for molecular characterisation over recent years. Specifically, there have been many instances where the chirality of molecules has been inferred from molecular packing[1-3] or has been imaged unambiguously with the STM.[4-6] However STM can also be used to view the starting materials and products of reactions on surfaces[7] and even to initiate them[8]. Many of the reactions occurring at solid surfaces involve a dissociation of the deposited molecular species. Here we focus on the adsorption and dissociation of a chiral ester on reactive and unreactive metallic substrates.

Ester cleavage is particularly important for a wide range of synthetic reactions, ranging from multitonne hydrolysis of fatty acids to form soap and detergents, to small scale applications in the pharmaceutical and specialist chemical sectors.[9] Depending on the reaction conditions used, the products can alter. For example, in pyrolysis the decomposition of esters with a β-hydrogen generates the carboxylic acid and complementary alkene[10] while in solution esters are hydrolysed to the corresponding carboxylic acid and alcohol by using a base. The introduction of heterogeneous catalytic mediators such as Rh has been shown to hydrogenolyse esters via cleavage of the R-OC(O)R bond, producing the acid and an alkane.[11] All of these methods generate an acid along with a separate fragment. However, it has been reported that if Cu is used as catalyst, esters are reduced to the two corresponding primary alcohols.[12] Theoretical modelling performed on heterogeneous Cu clusters[13] indeed showed a dissociative adsorption along the RO-C(O)R bond to generate the RO(Cu) and RC(Cu)O species which then undergo hydrogenation to generate the corresponding alcohols.[13]

Metallic single crystal surfaces are the ideal model systems to experimentally investigate heterogeneous catalytic reactions. To the best of our knowledge, only a few studies have dealt with the
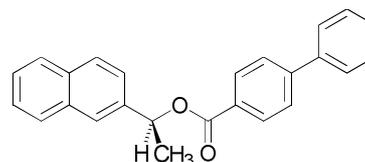
Scheme 1. (*S*)-1-(2'-naphthyl)ethyl-(4-phenylbenzoate) (NEP)

deposition of esters on model surfaces. Alkyl and phenyl esters adsorbed at the solid-liquid interface onto Au(111) did not show any type of dissociation.[14] Similarly, methylacetoacetate deposited in ultra high vacuum (UHV) onto Ni(111)[15] and Au(111)[16] remained intact. Also methyl acetate remained stable on Cu(110) unless the substrate was partially covered by oxygen where it was determined to react with oxygen atoms to generate methoxy and acetate fragments.[17] Only more recently, the dissociation of ester protected amines into alkenes and acids has been suggested as one of the steps in a complex reaction mechanism for the creation of surface confined polymers.[18]

In this Communication we report on the UHV deposition and STM analysis of a de-novo synthesised ester onto both Cu(110) and Au(111) substrates to directly image the products of dissociative adsorption thereby allowing us to elucidate the reaction pathway. The two surfaces were chosen as exemplary systems for reactive and unreactive substrates, respectively. The (*S*)-1-(2'-naphthyl)ethyl-(4-phenylbenzoate) molecule (NEP, scheme 1) was selected as a model system for investigating ester cleavage. NEP contains two structurally distinct extended aromatic ring systems either side of the ester, each of which has the potential to bind to a surface. The molecule is stable during thermal sublimation, the deposition technique used in this work, as shown by mass spectrometry. Full synthetic and sample preparation details are given in the electronic supporting information (ESI).

Upon adsorption of NEP at room temperature on Cu(110), oblong features appear which are oriented along the [001] and [1$\bar{1}$0] crystallographic directions of the substrate, figures 1(a) and (b). These features have two distinct lengths of 11.5 ± 0.4 Å and 12.6 ± 0.6 Å which are significantly smaller than the theoretical length of NEP, 18 Å. This reduced length is a first indication that the NEP molecules have adsorbed dissociatively. Cu(110) is known to be a very reactive substrate because of the high density of active sites exposed by its atomic-scale corrugation. For example,
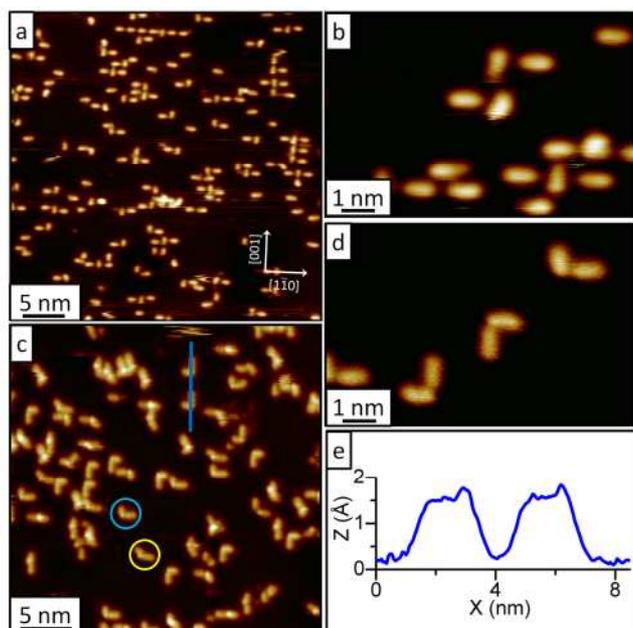
Fig 1. STM images of NEP deposited on Cu(110). (a) and (b), room temperature deposition, the observed features are the result of adsorption-induced fragmentation. (c) and (d), deposition at -130°C, corresponding to intact molecules. The two main conformations are circled in (c). (e) Linescan over the blue line in (c) showing the methyl protrusions. All images were acquired at -196°C.

it has been well documented that the room temperature adsorption of benzene-carboxylic acids onto Cu(110) can cause their deprotonation resulting in surface-stabilised negatively charged carboxylate species.[19-22]

A similar species, biphenyl carboxylate, is also one of the possible fragments of the NEP if its cleavage occurred at the RCH(CH$_3$)-OC(O)R bond. The cationic species resulting from this fragmentation is actually observed in the positive mode electrospray mass spectrum of NEP (figure ESI.1). This secondary cation is particularly stable in the case of NEP because it is situated next to the aromatic naphthalene group. If adsorbed on a metallic surface, the cation is however expected to deprotonate and transform to the corresponding 2-vinylnaphthalene alkene (see ESI). In order to confirm the nature of the fragments, a comparison was made with the biphenyl carboxylic acid molecule which is expected to deprotonate to the carboxylate upon adsorption on Cu(110).[19] The main assembly motifs observed for both dissociated NEP and biphenyl carboxylic acid are compared in the ESI (Figure ESI.3). All of the structures observed in the carboxylic acid sample are also present in the dissociated NEP and are explained by ionic H-bonding of the COO$^-$ to the aromatic hydrogens. Although a similar H-bonding motif could in theory be proposed also for the radical carbonyl fragment generated by cleavage of the RO-C(O)R bond, this would not fully explain the observed assemblies (figure ESI.4). As a consequence, we identify the longer of the two fragments described above as the carboxylate and thus infer that the molecule has cleaved along the RCH(CH$_3$)-OC(O)R bond.

The main difference between the dissociated NEP and the biphenylcarboxylic acid is the presence of many monomeric units in the former sample. Most of these fragments have the shorter of the two characteristic lengths described above, are asymmetric

and a detailed inspection reveals that they appear in two mirror symmetric forms (figure ESI.5). While the prochiral 2-vinylnaphthalene species generated by the cleavage of NEP at the RCH(CH$_3$)-OC(O)R bond can explain this appearance, a cleavage of the RO-C(O)R bond would produce a fully chiral 1-(2-naphthyl)ethanoyl species (ESI) which cannot take two mirror symmetric conformations. This is further proof that NEP actually dissociates along the RCH(CH$_3$)-OC(O)R bond.

To further investigate this dissociative adsorption, the effect of thermal activation on the reaction was studied by reducing the substrate temperature. Figure 1(c) shows the structures observed by depositing NEP on Cu(110) held at -130°C which are different from those observed at room temperature: Only 20% of the molecules have fragmented, while the remaining 80% are still intact. These latter appear as two lobes, one larger than the other, linked by a bright protrusion. The lobes can be assigned to the biphenyl and naphthalene rings (large and small lobe, respectively) while the protrusion (figure 1(e)) is identified as the methyl group oriented normal to the surface. Two main conformations are observed for the intact molecules; 45% of them have an L shape where the lobes are 90° to each other (highlighted by the blue circle in figure 1(c)), while in 35% of the cases the lobes are separated by 130° (yellow circle in figure 1(c)). This difference arises because of a rotation of 180° around the naphthalene – CCH$_3$O bond (figure ESI.7) and is a further indication that the molecules are indeed intact. Semi-empirical AM1 calculations show that in the gas phase these two configurations have identical energies (ESI). Thus, the different observed frequency of the two conformations must be due to the interaction with the substrate. The remaining 20% of the intact molecules have distinct conformations to these main two. Figure 1(d) shows a zoom of the single molecules where, however, the methyl groups are not imaged as protrusions. We attribute this imaging mode to a different tip state (ESI).[23]

Finally, in order to investigate the effect of the substrate chemistry on the fragmentation of NEP, similar experiments were also performed on the far less reactive Au(111) surface. Room temperature deposition on Au(111) resulted in the great majority of molecules adsorbing intact. In fact the NEP molecules arrange into chiral hierarchical supramolecular architectures, figure 2(a), where the individual molecules are imaged in the same manner as on the low temperature Cu(110). The first level of the hierarchical order is formed by H-bonding of individual molecules to organise their smaller lobes into a triangle, while the longer lobes point perpendicular to its sides. This arrangement is highlighted by a blue outline in figure 2(b). Further packing of the stars into a second level of hierarchy, generates larger supramolecular domains, typically extending over 15-20nm. The arrangement of the stars always follows the same rotation, indicating that the chirality of the NEP molecule is propagated throughout the hierarchical assembly. Annealing of the sample does not generate larger domains and, above 100°C, induces desorption of the majority of the molecules. The few remaining structures are supramolecular arrangements that maintain a triangular symmetry but also include molecular fragments, figure 2(c). Three fragments orient in a chiral manner to form a three-pronged star which also includes three intact molecules arranged between the prongs, figure 2(d). All of these structures display
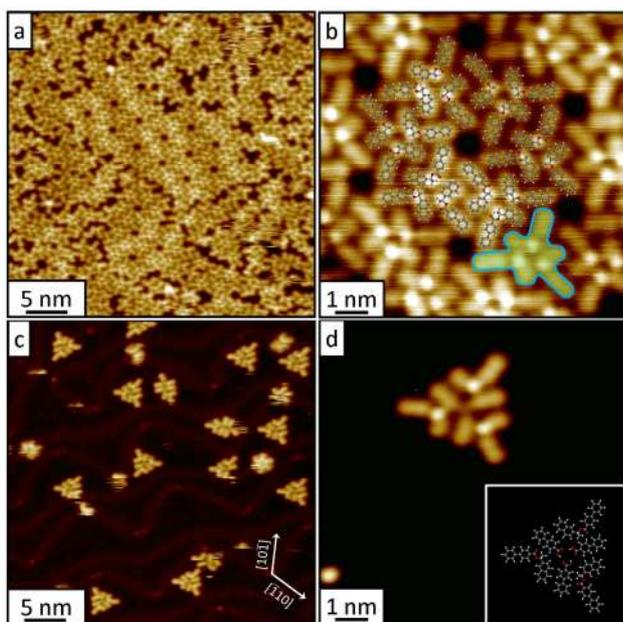
Fig 2. STM image of NEP deposited onto Au(111). (a) and (b), room temperature deposition. (b) Zoom of the triangular structures in (a) with overlaid molecular model of the packing. The blue outline highlights a single six-pronged star. (c) and (d), effect of annealing to 100°C; the coverage is reduced and the structures are composed of both whole molecules and molecular fragments. (d) Zoom of an individual triangular cluster from (c) with proposed model inset. All images were acquired at -196°C.

the same chirality and are aligned with the fragments along the $[10\bar{1}]$ directions of the surface. As a consequence, only two 60° mutually rotated orientations are possible. A few features involving just the fragment species are also observed, such as two three-pronged stars joined together or a six-pronged chiral propeller displaying both *R*- and *S*-organisational chiralities. We note that all of these structures can also be found in small percentages on the room temperature high coverage sample, indicating that Au(111) still has residual catalytic activity although significantly lower than that of Cu(110).

Also for Au(111) the nature of the fragments was investigated by a comparative room temperature deposition of the biphenylcarboxylic acid molecule. The corresponding STM measurements show assemblies similar to the structures formed by the NEP fragments as, for example, the three pronged stars (figure ESI.10).

The fact that for both Cu(110) and Au(111) the STM images of the NEP fragments appear very similar to the images obtained by depositing the biphenylcarboxylic acid allows us to delineate a hypothesis for the reaction mechanism. In particular, on room temperature Cu(110) the acid is stable only in its deprotonated form[19-21], implying by comparison that the ester is being cleaved at the RCH(CH_3)-OC(O)R bond to form the carboxylate and the cation, the latter most probably further deprotonating to an alkene. On the other hand, the biphenylcarboxylic acid molecule is not expected to deprotonate on Au(111) which means that also the fragment must be in its acidic form on this surface. We therefore tentatively suggest that on Au(111) NEP initially fragments as on Cu(110) but that the proton released from the transformation of the cation to the alkene, instead of recombining

and desorbing as molecular hydrogen, is transferred via the substrate to the nearby carboxylate fragment, turning it into the acid species (ESI). A concerted β-H elimination pathway could also occur, although this is expected to be less likely because of the molecular conformation of NEP on the surface.

Our measurements clearly show that on both surfaces the ester dissociates along the RCH(CH_3)-OC(O)R bond. This is different from what was reported for heterogeneous Cu catalysis[11] and from the dissociation pathway suggested by calculations[12] but agrees with the suggested pathway for Boc-removal proposed in reference [18]. Possible reasons for this could be the strength of the interaction of the carboxylate/carboxylic moieties with the Cu(110)/Au(111) surfaces, which are different from the Cu clusters used in the calculation, or the stability of the specific NEP cationic fragment after dissociation.

In conclusion, we have shown that the ester NEP dissociates at room temperature on Cu(110) and at high temperature on Au(111) but remains largely intact on low temperature Cu(110) and room temperature Au(111), where it generates a chiral hierarchical supramolecular structure. The products of dissociation have been clearly identified by comparison with biphenylcarboxylic acid. Based on this, we have demonstrated that on both surfaces the ester cleavage occurs along the RCH(CH_3)-OC(O)R bond. Moreover, we propose that an effective proton transfer takes place on Au(111) to generate the acid and complementary alkene after the initial bond cleavage.

Notes and references

a Department of Chemistry, University of Warwick, Gibbet Hill Road, Coventry, CV4 7AL, UK. E-mail: g.costantini@Warwick.ac.uk; Tel: +44 24 765 24934

1. S. Haq, et al., *Nature Chem.*, 2009, **1**, 409-414.
2. M. Lingenfelder, et al., *Angew. Chem. Int. Ed.*, 2007, **46**, 4492-4495.
3. K.-H. Ernst, in *Supramolecular Chirality*, eds. M. CregoCalama and D. N. Reinboudt, 2006, vol. 265, pp. 209-252.
4. V. Demers-Carpentier, et al., *Science*, 2011, **334**, 776-780.
5. F. Masini, et al., *J. Am. Chem. Soc.*, 2011, **133**, 13910-13913.
6. S. De Feyter, et al., *Langmuir*, 1999, **15**, 2817-2822.
7. G. Franc and A. Gourdon, *PCCP*, 2011, **13**, 14283-14292.
8. S. W. Hla, et al., *Phys. Rev. Lett.*, 2000, **85**, 2777-2780.
9. J. S. Carey, et al., *Org. Biomol. Chem.*, 2006, **4**, 2337-2347.
10. A. Maccoll, in *Adv. Phys. Org. Chem.*, ed. V. Gold, Academic Press, 1965, vol. Volume 3, pp. 91-122.
11. M. Zdrazil and M. Kraus, *Collect. Czech. Chem. Commun.*, 1974, **39**, 3515-3521.
12. J. W. Evans, et al., *J. Catal.*, 1984, **88**, 203-213.
13. M. A. N. Santiago, et al., *J. Catal.*, 2000, **193**, 16-28.
14. K. Tahara, et al., *CrystEngComm*, 2011, **13**, 5551-5558.
15. T. E. Jones and C. J. Baddeley, *Surf. Sci.*, 2002, **519**, 237-249.
16. A. G. Trant and C. J. Baddeley, *Langmuir*, 2011, **27**, 1788-1795.
17. S. L. Silva, et al., *Surf. Sci.*, 2000, **452**, 79-94.
18. S. Boz, et al., *Angew. Chem. Int. Ed.*, 2009, **48**, 3179-3183.
19. B. G. Frederick, et al., *Surf. Sci.*, 1993, **292**, 33-46.
20. D. S. Martin, et al., *Physical Review B*, 2002, **66**, 155427.
21. T. Classen, et al., *J. Phys. Chem. A*, 2007, **111**, 12589-12603.
22. Y. Wang, et al., *Chem. Commun.*, 2012, **48**, 534-536.
23. M. M. Knudsen, et al., *J. Am. Chem. Soc.*, 2011, **133**, 4896-4905.